

Syntheses and molecular structures of novel Ru(II) complexes with bidentate benzimidazole based ligands and their catalytic efficiency for oxidation of benzyl alcohol

Osman Dayan ^{a,*}, Melek Tercan ^a, Namik Özdemir ^b

^a Department of Chemistry, Faculty of Arts and Sciences, Çanakkale Onsekiz Mart University, 17020, Çanakkale, Turkey

^b Department of Secondary School Science and Mathematics Education, Faculty of Education, Ondokuz Mayıs University, 55139, Samsun, Turkey



ARTICLE INFO

Article history:

Received 21 December 2015

Received in revised form

2 May 2016

Accepted 4 June 2016

Available online 7 June 2016

Keywords:

Ru (II) complexes

Piano-stool complexes

Oxidation of benzyl alcohol

Bidentate chelates

2-(2-quinolinyl)-1H-benzimidazole

ABSTRACT

Five bidentate ligands derived from quinoline-2-carboxylic acid, i.e. 2-(1H-benzimidazol-2-yl)quinoline (**L1**), 2-(1-benzyl-1H-benzimidazol-2-yl)quinoline (**L2**), 2-[1-(2,3,5,6-tetramethylbenzyl)-1H-benzimidazol-2-yl]quinoline (**L3**), 2-[1-(4-chlorobenzyl)-1H-benzimidazol-2-yl]quinoline (**L4**), and 2-[1-(4-methylbenzyl)-1H-benzimidazol-2-yl]quinoline (**L5**) were synthesized. Treatment of **L1–L5** with [RuCl₂(*p*-cymene)]₂ and KPF₆ afforded six-coordinate piano-stool Ru(II) complexes, namely, [RuCl(**L1**)(*p*-cymene)]PF₆ (**C1**), [RuCl(**L2**)(*p*-cymene)]PF₆ (**C2**), [RuCl(**L3**)(*p*-cymene)]PF₆ (**C3**), [RuCl(**L4**)(*p*-cymene)]PF₆ (**C4**), and [RuCl(**L5**)(*p*-cymene)]PF₆ (**C5**). Synthesized compounds were characterized with different techniques such as ¹H and ¹³C NMR, FT-IR, and UV-vis spectroscopy. The solid state structure of **L1** and **C3** was confirmed by single-crystal X-ray diffraction analysis. The single crystal structure of **C3** verified coordination of **L3** to the Ru(II) center. The Ru(II) center has a pseudo-octahedral three legged piano stool geometry. The complexes **C1–C5** were tested as catalysts for the catalytic oxidation of benzyl alcohol to benzaldehyde in the presence of periodic acid (H₅IO₆) (Substrate/Catalyst/Oxidant = 1/0.01/0.5). The best result was obtained with **C2** (3 h → 90%).

© 2016 Elsevier B.V. All rights reserved.

1. Introduction

It is known that ruthenium (II) complexes are the most useful catalysts for many reactions [1–5]. Complexes of Ru containing π -acceptor nitrogen-bearing ligands, especially N-heteroaromatic systems like pyridyl-based benzimidazolyl ligands have been widely studied. The pyridine ring as a good π -acceptor tends to stabilize the Ru(II) acceptor center and the imidazole and its derivatives exhibit moderate π -donor properties [6]. Thus the steric and electronic properties around the metal centre can be changed with benzimidazole type ligands.

Benzimidazoles have attracted much attention due to their usage in many applications in coordination-, medicinal- and supramolecular-chemistry [7–12]. Because of having high thermal stability, good catalytic performance and superior optical properties, metal complexes with benzimidazole ligands are important [13–20]. Recently, many efficient Ru(II) complexes of

benzimidazole ligands have been reported as catalysts [17,18,21–23]. Related transition metal complexes containing 2-(2'-quinolyl)benzimidazoles are very rare. However, some researchers show that their related Ni, Cu, Ir, Re, Pd, Ti, Zn and Ru complexes have good optoelectronic and catalytic properties [24–33]. To our best knowledge, there is only one ruthenium complex with a similar ligand [30].

Because of restricted raw material supplies, developments of new catalysts for the selective oxidation of benzyl alcohol to benzaldehyde are important from the environmental perspective [34]. Traditional methods usually need stoichiometric amounts of oxidants such as manganese and chromium oxides which are hazardous [5]. Many materials were synthesized and tested for oxidation of benzyl alcohol to benzaldehyde as homogeneous or heterogeneous catalysts to date [35–39]. But, ruthenium-based homogenous catalysts are relatively rare in this field [40]. The oxido-ruthenium species, which are formed from ruthenium (II/III) complexes by using various oxidants, make the oxygen-transfer reactions possible. Many mono- and dinuclear-Ru complexes of tpa-based ligands have attracted interest for catalytic oxidation reactions and have shown high catalytic efficiency towards alkene

* Corresponding author.

E-mail address: osmandayan@comu.edu.tr (O. Dayan).

oxygenation of unsaturated hydrocarbons [41].

In this work, we synthesized 2-(2'-quinolyl)benzimidazole type ligands and the Ru complexes of these ligands. All of the synthesized compounds were characterized by ^1H and ^{13}C NMR, IR and UV-visible spectroscopic techniques. Then their catalytic activities in the selective oxidation of benzyl alcohol to benzaldehyde were investigated.

2. Experimental

Chemicals were obtained from commercial suppliers and used as purchased. **L1** [42] was synthesized using the method in the published procedure. Information about techniques and devices used are given in [supporting information](#).

2.1. Synthesis of ligands

2.1.1. Synthesis of 2-(1H-benzimidazol-2-yl)quinoline (**L1**)

Quinaldic acid (10 mmol, 1.731 g) and *o*-phenylenediamine (10 mmol, 1.081 g) were stirred in polyphosphoric acid (20 mL) for 4 h at 200 °C under argon. At the end this time, the green-colored molten fluid was poured into iced water. Then the solution was neutralized with ammonium hydroxide and the obtaining solid was filtered off. Finally, the product was recrystallized by EtOH.

Beige solid, 84% yield, m. p.: 238 °C. ^1H NMR (600 MHz, DMSO- d_6 , δ ppm): 7.25 (1 H, t, J = 7.52 Hz, - H_d); 7.30 (1 H, t, J = 7.70 Hz, - H_5); 7.63 (1 H, d, J = 7.70 Hz, - H_3); 7.67 (1 H, ddd, J = 8.07, 6.79 and 1.28 Hz, - H_{13}); 7.77 (1 H, d, J = 8.07 Hz, - H_6); 7.86 (1 H, ddd, J = 8.44, 6.97 and 1.47 Hz, - H_{14}); 8.06 (1 H, dd, J = 8.07 and 1.47 Hz, - H_{10}); 8.17 (1 H, dd, J = 8.25 and 0.92 Hz, - H_9); 8.49 (1 H, d, J = 8.4 Hz, - H_{12}); 8.54 (1 H, d, J = 8.4 Hz, - H_{15}); 13.22 (1 H, s, -NH). ^{13}C NMR (150.92 MHz, DMSO- d_6 , δ ppm): 112.27; 119.20; 119.55; 122.05; 123.58; 127.28; 128.06; 128.22; 128.73; 130.44; 135.18; 137.39; 143.92; 147.18; 148.71 (- C_8); 150.70 (- C_1). FTIR (ν/cm^{-1}): 3482, 3056, 1948, 1930, 1890, 1852, 1810, 1655, 1597, 1564, 1537, 1497, 1444, 1414, 1318, 1105, 830, 741. UV-Vis (nm): 242, 287, 323, 345 ($\pi \rightarrow \pi^*$ and $n \rightarrow \pi^*$).

2.1.2. General procedure for the synthesis of **L2–5**

L1 (2.04 mmol, 0.500 g) and KOH (2.04 mmol, 0.114 g) were stirred at 150 °C in DMF for 4 h. Then, appropriate substituted-benzyl halides (2.04 mmol) were added to the reaction mixture and further stirred at 150 °C for 24 h. Volatiles were distilled under vacuum and the remaining solid was washed with water and recrystallized with MeOH.

2.1.2.1. Data for 2-(1-benzyl-1H-benzimidazol-2-yl)quinoline (L2**)** Yellowish brown solid, 82% yield, m.p.: 145 °C. ^1H NMR (600 MHz, DMSO- d_6 , δ ppm): 6.41 (2 H, s, - H_a); 7.15 (1 H, dq, J = 8.62 and 4.34 Hz, - H_e); 7.21–7.23 (4 H, m, - $H_{3,4,5,6}$); 7.32 (2 H, dddd, J = 15.96, 7.24, 7.06 and 1.28 Hz, - H_d); 7.65 (1 H, ddd, J = 8.07, 6.97 and 1.10 Hz, - H_{13}); 7.69 (1 H, dd, J = 6.79 and 1.28 Hz, - H_{10}); 7.79 (1 H, ddd, J = 8.44, 6.97 and 1.47 Hz, - H_{14}); 7.83 (1 H, dd, J = 8.07 and 1.10 Hz, - H_9); 8.02 (2 H, dt, J = 8.16 and 1.79 Hz, - H_c); 8.50–8.55 (2 H, m, - $H_{12,15}$). ^{13}C NMR (150.92 MHz, DMSO- d_6 , δ ppm): 48.37 (- C_a); 111.32; 119.88; 121.33; 122.74; 123.87; 126.66; 127.09; 127.34; 127.57; 127.95; 128.44; 128.97; 130.29; 136.99; 137.09; 138.11; 142.17; 146.44; 148.78 (- C_8); 149.91 (- C_1). FTIR (ν/cm^{-1}): 3050, 3024, 2987, 1613, 1596, 1562, 1493, 1453, 1433, 1401, 1356, 1327, 1164, 842, 717. UV-Vis (nm): 218, 243, 285, 333 ($\pi \rightarrow \pi^*$ and $n \rightarrow \pi^*$).

2.1.2.2. Data for 2-[1-(2,3,5,6-tetramethylbenzyl)-1H-benzimidazol-2-yl]quinoline (L3**)** White solid, 72% yield, m.p.: 166 °C. ^1H NMR (600 MHz, DMSO- d_6 , δ ppm): 1.78–2.26 (12 H, m, - CH_3); 6.49 (2 H, s, - H_a); 6.67–6.84 (1 H, m, - H_d); 6.92 (1 H, s, - H_e); 6.99–7.11 (1 H, m,

- H_5); 7.15–7.19 (1 H, m, - H_{13}); 7.59–7.77 (2 H, m, - $H_{3,6}$); 7.81–7.84 (1 H, m, - H_{14}); 8.00–8.23 (2 H, m, - $H_{9,10}$); 8.42 (1 H, m, - H_{12}); 8.53–8.57 (1 H, m, - H_{15}). ^{13}C NMR (150.92 MHz, DMSO- d_6 , δ ppm): 15.98 (- CH_3); 20.61 (- CH_3); 46.61 (- C_a); 112.22; 120.33; 122.49; 122.64; 123.87; 127.77; 128.12; 128.48; 129.62; 130.77; 131.78; 133.07; 133.78; 133.99; 136.95; 137.57; 142.82; 146.76; 150.30 (- C_8); 151.27 (- C_1). FTIR (ν/cm^{-1}): 3480, 3052, 3007, 2973, 2949, 2923, 2866, 1614, 1595, 1560, 1496, 1439, 1328, 1166, 846, 739. UV-Vis (nm): 204, 244, 285, 349 ($\pi \rightarrow \pi^*$ and $n \rightarrow \pi^*$).

2.1.2.3. Data for 2-[1-(4-chlorobenzyl)-1H-benzimidazol-2-yl]quinoline (L4**)** White solid, 78% yield, m.p.: 188 °C. ^1H NMR (600 MHz, DMSO- d_6 , δ ppm): 6.40 (2 H, s, - H_a); 7.26–7.29 (2 H, m, - H_c); 7.31–7.39 (4 H, m, - $H_{3,4,d}$); 7.68 (1 H, ddd, J = 8.07, 6.97 and 1.10 Hz, - H_5); 7.70–7.75 (1 H, m, - H_{13}); 7.82 (1 H, ddd, J = 8.34, 6.69 and 1.47 Hz, - H_{14}); 7.85 (1 H, dd, J = 6.97 and 1.10 Hz, - H_6); 8.02 (1 H, d, J = 7.70 Hz, - H_9); 8.05 (1 H, dd, J = 8.25 and 0.92 Hz, - H_{10}); 8.52–8.57 (2 H, m, - $H_{12,15}$). ^{13}C NMR (150.92 MHz, DMSO- d_6 , δ ppm): 47.86 (- C_a); 111.21; 119.94; 121.28; 122.85; 123.99; 127.37; 127.63; 127.97; 128.46; 128.54; 128.98; 130.34; 131.68; 136.89; 137.22; 142.15; 146.43; 148.69 (- C_8); 149.76 (- C_1). FTIR (ν/cm^{-1}): 3052, 2998, 2947, 1951, 1922, 1895, 1615, 1600, 1564, 1510, 1490, 1459, 1442, 1328, 1078, 833, 738. UV-Vis (nm): 206, 244, 285, 334, 349 ($\pi \rightarrow \pi^*$ and $n \rightarrow \pi^*$).

2.1.2.4. Data for 2-[1-(4-methylbenzyl)-1H-benzimidazol-2-yl]quinoline (L5**)** White solid, 82% yield, m.p.: 157 °C. ^1H NMR (400 MHz, CDCl₃, δ ppm): 2.31 (3 H, s, - CH_3); 6.28–6.42 (2 H, m, - H_a); 7.12 (2 H, d, J = 6.87 Hz, - H_c); 7.23–7.40 (4 H, m, - $H_{3,4,d}$); 7.74 (1 H, dd, J = 9.39 and 2.52 Hz, - H_6); 7.96 (1 H, t, J = 7.56 Hz, - H_5); 8.14–8.21 (2 H, m, - $H_{10,13}$); 8.22–8.28 (1 H, m, - H_{14}); 8.39 (1 H, d, J = 8.70 Hz, - H_9); 8.83–8.88 (1 H, m, - H_{12}); 8.93 (1 H, d, J = 9.16 Hz, - H_{15}). ^{13}C NMR (100.53 MHz, CDCl₃, δ ppm): 20.98 (- CH_3); 48.94 (- C_a); 110.75; 120.24; 121.74; 122.82; 123.84; 126.81; 127.21; 127.59; 127.69; 129.18; 129.58; 129.68; 134.59; 136.53; 136.88; 137.11; 142.12; 149.61 (- C_8); 150.24 (- C_1). FTIR (ν/cm^{-1}): 3053, 2963, 2925, 1612, 1599, 1563, 1509, 1497, 1459, 1445, 1329, 1076, 742, 736. UV-Vis (nm): 218, 243, 285, 334, 349 ($\pi \rightarrow \pi^*$ and $n \rightarrow \pi^*$).

2.2. General procedure for the synthesis of [RuCl(**L1–5**)(*p*-simen)]PF₆

The appropriate ligand (**L1–5**) (0.320 mmol) and [RuCl(*p*-cymene)]₂ (0.160 mmol, 0.100 g) were refluxed in ethanol for 8 h. At the end of this time, the mixture was cooled at room temperature and precipitated by addition of diethyl ether. The soluble part of this precipitate in water was treated with saturated KPF₆ solution. The precipitate was filtered off, washed and dried.

2.2.1. Data for [RuCl(**L1**)(*p*-cymene)]PF₆ (**C1**)

Reddish brown, 95% yield, m.p. > 280 °C. ^1H NMR (400 MHz, DMSO- d_6 , δ ppm): 0.72 (6 H, dd, J = 17.63 and 7.10 Hz, - H_o); 2.18–2.22 (1 H, m, - H_n); 2.29 (3 H, s, - H_k); 6.12 (1 H, d, J = 5.95 Hz, - H_l); 6.26 (1 H, d, J = 5.95 Hz, - H_l); 6.33 (2 H, dd, J = 11.91 and 6.41 Hz, - H_m); 7.61–7.70 (2 H, m, - $H_{3,4}$); 7.90–7.95 (1 H, m, - H_6); 7.98 (1 H, t, J = 7.33 Hz, - H_5); 8.17–8.21 (2 H, m, - $H_{10,13}$); 8.30 (1 H, m, - H_{14}); 8.53 (1 H, d, J = 8.24 Hz, - H_g); 8.83 (1 H, d, J = 9.16 Hz, - H_{12}); 8.99 (1 H, d, J = 8.24 Hz, - H_{15}). ^{13}C NMR (100.53 MHz, DMSO- d_6 , δ ppm): 18.49 (- C_k); 21.16 (- C_o); 21.69 (- C_o); 30.32 (- C_n); 78.73; 83.70; 84.20; 85.20; 102.75; 104.71; 114.34; 118.13; 118.63; 125.42; 126.60; 128.88; 129.31; 129.37; 129.55; 133.30; 134.33; 141.53; 141.72; 147.57; 148.58; 149.98. FTIR (ν/cm^{-1}): 3186, 3081, 2973, 2940, 2883, 1620, 1593, 1547, 1509, 1474, 1450, 1431, 1395, 1380, 1326, 1029, 828, 748, 556, 520. UV-GB (nm): 216, 249, 305 ($\pi \rightarrow \pi^*$ and $n \rightarrow \pi^*$), 382 [Ru(d π) \rightarrow π^* (MLCT)].

2.2.2. Data for [RuCl(L2)(p-cymene)]PF₆ (**C2**)

Brown, 89% yield, m.p.> 280 °C. ¹H NMR (400 MHz, DMSO-d₆, δ ppm): 0.62 (3 H, d, *J* = 6.87 Hz, -H₀); 0.74 (3 H, d, *J* = 6.87 Hz, -H₀); 2.08–2.19 (1 H, m, -H_n); 2.31 (3 H, s, -H_k); 6.21–6.46 (6 H, m, -H_{l,m,a}); 7.12 (2 H, d, *J* = 7.33 Hz, -H_c); 7.27–7.37 (3 H, m, -H_{3,4,5}); 7.71–7.77 (2 H, m, -H_d); 7.96 (1 H, t, *J* = 7.56 Hz, -H_e); 8.12–8.31 (4 H, m, -H_{6,10,13,14}); 8.39 (1 H, d, *J* = 8.70 Hz, -H₁₂); 8.85 (1 H, d, *J* = 8.70 Hz, -H₉); 8.93 (1 H, d, *J* = 9.16 Hz, -H₁₅). ¹³C NMR (100.53 MHz, DMSO-d₆, δ ppm): 18.42 (-C_k); 20.97 (-C₀); 21.92 (-C₀); 30.22 (-C_n); 48.31 (-C_a); 84.82; 85.00; 85.22; 85.57; 112.98; 118.84; 119.82; 125.77; 125.80; 126.22; 127.21; 128.46; 128.93; 129.18; 129.76; 129.94; 133.27; 135.42; 136.50; 140.47; 141.12; 146.98; 148.23; 149.42. FTIR (ν/cm⁻¹): 3073, 2969, 2922, 2879, 1616, 1594, 1527, 1499, 1478, 1454, 1428, 1378, 1101, 831, 761. UV–Vis (nm): 213, 252, 305 (π→π* and n→π*), 372 [Ru(dπ)→π* (MLCT)].

2.2.3. Data for [RuCl(L3)(p-cymene)]PF₆ (**C3**)

Reddish brown, 92% yield, m.p.> 280 °C. ¹H NMR (600 MHz, DMSO-d₆, δ ppm): 0.68 (3 H, d, *J* = 6.97 Hz, -H₀); 0.82 (3 H, d, *J* = 6.97 Hz, -H₀); 1.98 (6 H, s, -CH₃, benzyl); 2.19 (7 H, br. s., -CH₃, benzyl and -H_n); 2.29 (3 H, s, -H_k); 5.67–6.34 (6 H, m, H_{l,m,a}); 6.43 (1 H, m, -H₃); 6.72 (1 H, d, *J* = 8.44 Hz, -H₆); 7.10 (1 H, s, -H_e); 7.36 (1 H, t, *J* = 8.07 Hz, -H₁₄); 7.55 (1 H, t, *J* = 7.70 Hz, -H₄); 8.00 (1 H, t, *J* = 7.52 Hz, -H₅); 8.13 (1 H, d, *J* = 8.07 Hz, -H₁₂); 8.20 (1 H, t, *J* = 7.89 Hz, -H₁₃); 8.34 (1 H, d, *J* = 8.07 Hz, -H₉); 8.86 (1 H, d, *J* = 8.80 Hz, -H₁₀); 8.98 (1 H, m, -H₁₅). ¹³C NMR (150.92 MHz, DMSO-d₆, δ ppm): 15.38 (-CH₃, benzyl); 18.39 (-C_k); 20.09 (-CH₃, benzyl); 20.87 (-C₀); 22.09 (-C₀); 30.32 (-C_n); 48.43 (-C_a); 84.86; 85.11; 85.48; 86.34; 113.45; 118.91; 119.19; 119.84; 121.28; 125.37; 126.32; 128.46; 128.90; 129.83; 130.30; 132.42; 133.08; 133.28; 133.80; 134.04; 135.48; 140.68; 147.74; 149.30; 149.59. FTIR (ν/cm⁻¹): 3079, 2963, 2939, 2882, 1619, 1594, 1572, 1529, 1509, 1474, 1430, 1414, 1380, 1062, 1029, 828, 748, 660. UV–Vis (nm): 216, 245, 306, 351 (π→π* and n→π*), 382 [Ru(dπ)→π* (MLCT)].

2.2.4. Data for [RuCl(L4)(p-cymene)]PF₆ (**C4**)

Brown, 83% yield, m.p.> 280 °C. ¹H NMR (600 MHz, DMSO-d₆, δ ppm): 0.63 (3 H, d, *J* = 6.97 Hz, -H₀); 0.75 (3 H, d, *J* = 6.97 Hz, -H₀); 2.12–2.16 (1 H, m, -H_n); 2.30 (3 H, s, -H_k); 5.99 (1 H, d, *J* = 5.87 Hz, -H_l); 6.26 (1 H, d, *J* = 6.24 Hz, -H_m); 6.29 (1 H, d, *J* = 6.24 Hz, -H_m); 6.31–6.35 (2 H, m, -H_a); 6.39 (1 H, d, *J* = 5.87 Hz, -H_l); 7.16 (2 H, d, *J* = 8.80 Hz, -H_c); 7.42 (2 H, d, *J* = 8.80 Hz, -H_d); 7.72–7.78 (2 H, m, -H_{3,4}); 7.97 (1 H, t, *J* = 7.70 Hz, -H₁₃); 8.15–8.20 (2 H, m, -H_{5,6}); 8.23–8.28 (2 H, m, -H_{12,14}); 8.40 (1 H, d, *J* = 8.80 Hz, -H₁₀); 8.87 (1 H, d, *J* = 8.44 Hz, -H₉); 8.93 (1 H, d, *J* = 8.80 Hz, -H₁₅). ¹³C NMR (150.92 MHz, DMSO-d₆, δ ppm): 18.88 (-C_k); 21.41(-C₀); 22.44 (-C₀); 30.70 (-C_n); 48.24 (-C_a); 80.42; 85.36; 86.00; 86.87; 113.44; 119.37; 120.31; 126.76; 127.75; 128.31; 129.01; 129.61; 130.27; 130.43; 133.25; 133.78; 135.00; 136.91; 137.75; 140.98; 141.72; 147.36; 148.68; 149.95. FTIR (ν/cm⁻¹): 3076, 2954, 2917, 2891, 2842, 1659, 1641, 1591, 1551, 1545, 1435, 1312, 1055, 821, 747, 692. UV–Vis (nm): 253, 305 (π→π* and n→π*), 373 [Ru(dπ)→π* (MLCT)].

2.2.5. Data for [RuCl(L5)(p-cymene)]PF₆ (**C5**)

Brown, 78% yield, m.p.> 280 °C. ¹H NMR (400 MHz, DMSO-d₆, δ ppm): 0.63 (3 H, d, *J* = 6.87 Hz, -H₀); 0.74 (3 H, d, *J* = 6.87 Hz, -H₀); 2.10–2.17 (1 H, m, -H_n); 2.22 (3 H, s, -H_k); 2.31 (3 H, s, -CH₃, benzyl); 5.98 (1 H, d, *J* = 5.95 Hz, -H_l); 6.17–6.41 (5 H, m, -H_{l,m,a}); 7.01 (2 H, d, *J* = 8.24 Hz, -H_c); 7.14 (2 H, d, *J* = 7.79 Hz, -H_d); 7.71–7.77 (2 H, m, -H_{3,4}); 7.96 (1 H, t, *J* = 7.56 Hz, -H₁₃); 8.13–8.19 (2 H, m, -H_{12,14}); 8.23–8.28 (2 H, m, -H_{5,6}); 8.39 (1 H, d, *J* = 8.70 Hz, -H₁₀); 8.85 (1 H, d, *J* = 8.70 Hz, -H₉); 8.93 (1 H, d, *J* = 8.70 Hz, -H₁₅). ¹³C NMR (100.53 MHz, DMSO-d₆, δ ppm): 18.42 (-C_k); 20.57 (-CH₃, benzyl); 21.89 (-C₀); 30.71(-C_n); 48.14 (-C_a); 80.24; 80.29; 85.35; 86.07; 112.97; 118.82; 119.87; 125.75; 126.19; 127.17; 128.46; 128.93;

129.69; 129.75; 129.92; 132.37; 133.25; 136.49; 137.51; 140.46; 141.11; 146.99; 148.21; 149.42. FTIR (ν/cm⁻¹): 3660, 3070, 2969, 2928, 2878, 1616, 1594, 1527, 1499, 1478, 1454, 1428, 1378, 1101, 831, 761. UV–Vis (nm): 213, 252, 305 (π→π* and n→π*), 372 [Ru(dπ)→π* (MLCT)].

2.3. Oxidation of benzyl alcohol

In a typical reaction, a test tube was filled with benzyl alcohol (1 mmol), periodic acid (0.5 mmol), **C1-5** (0.01 mmol) and CH₃CN (5 ml). This tube was refluxed for the appropriate time. The reactions were monitored by gas chromatography.

2.4. X-ray analysis

Intensity data of the compounds were collected on a STOE IPDS II diffractometer at room temperature using graphite-monochromated Mo Kα radiation by applying the ω-scan method. The structures were solved by direct methods using SHELXS-2013 [43] and refined with full-matrix least-squares calculations on *F*² using SHELXL-2014 [43] implemented in WinGX [44] program suite. All carbon bound H atoms were placed geometrically and treated using a riding model, fixing the bond lengths at 0.93, 0.98, 0.97 and 0.96 Å for aromatic CH, methine CH, CH₂ and CH₃ atoms, respectively. In **L1**, the hydrogen atoms of NH and OH₂ groups were located on a difference Fourier map and refined isotropically subject to DFIX restraints of N–H = 0.86 Å and O–H = 0.82 Å. The displacement parameters of the H atoms were fixed at *U*_{iso}(H) = 1.2*U*_{eq} (1.5*U*_{eq} for methyl and water) of their parent atoms. The crystal of **L1** was twinned and the final structure was refined as a 2-component twin with a refined value for the minor twin fraction of 0.469(4)%. The twinning matrix corresponds to (0, -1, 0; -1, 0, 0; 0, 0, -1). In **C3**, one of the hexafluorophosphate anions in the asymmetric unit is disordered about an inversion center and refined with occupancy of all atoms fixed at 0.5. The poor quality of the crystals and the additional presence of twinning in **L1** led to relatively high *R*-values. In the final difference Fourier map of the compounds, the highest residual electron density located 0.99 Å from atom H9A in **L1** and 1.15 Å from atom F8 in **C3** was essentially meaningless. Data collection: X-AREA [45], cell refinement: X-AREA, data reduction: X-RED32 [45]. Crystal data, data collection and structure refinement details are summarized in Table 1. PLATON [46] was used for the structural analysis and presentation of the results.

3. Results and discussion

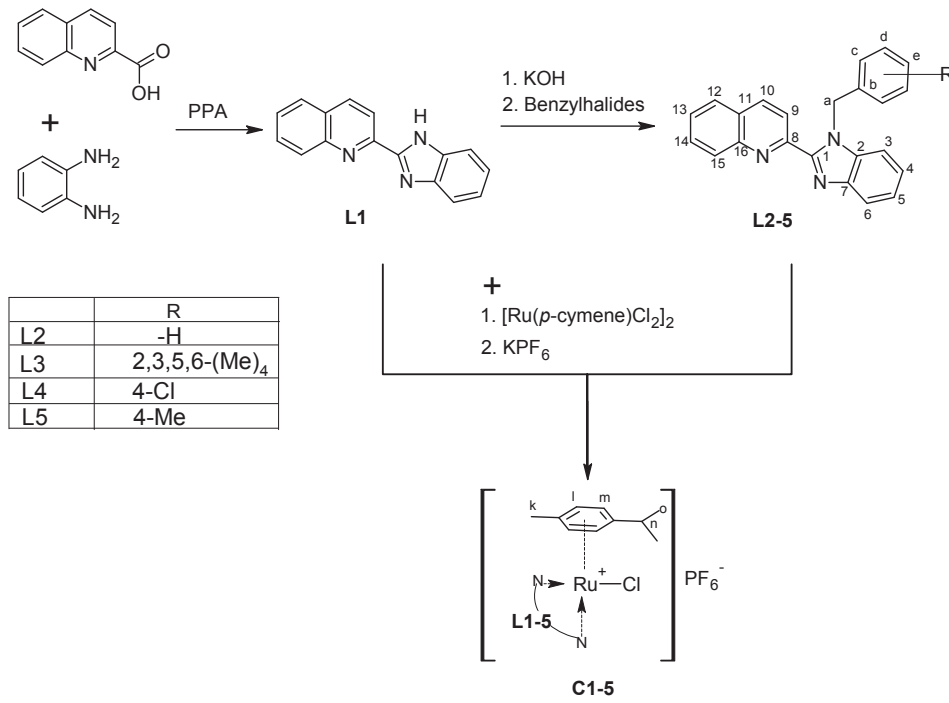
3.1. Synthesis and characterization of compounds

In this work, 2-(2-Quinolinyl)-1H-benzimidazole (**L1**) was synthesized by the reaction of quinaldic acid and o-phenylenediamine in polyphosphoric acid at 200 °C with high yields. N-substitution products (**L2-5**) of **L1** were achieved in the presence of KOH with different benzylhalides. The Ru(II) complexes of **L1-5** were prepared from the reaction of [Ru(p-cymene)Cl₂]₂, **L1-5** and KPF₆ (Scheme 1). All compounds (**L1-5** and **C1-5**) were soluble in many solvents such as EtOH, MeOH, DMF, DMSO and CH₂Cl₂. Synthesized compounds were characterized by ¹H and ¹³C NMR, FT-IR and UV-vis. All spectra of compounds are given in supporting information. Furthermore, solid state structure of **L1** and **C3** was determined by single crystal-X-ray diffraction.

In ¹H NMR spectra of **L1**, aromatic protons were seen at various peaks around 7.25–8.54 ppm. –H₄ and –H₅ protons on benzimidazol fragment of **L1** observed as triplet at 7.25 and 7.30 ppm, respectively. The other two protons from the benzimidazol

Table 1Crystal data and structure refinement parameters for **L1** and **C3**.

Parameter	L1	C3
CCDC depository	1036751	1036752
Color/shape	Colorless/prism	Orange/prism
Chemical formula	C ₁₆ H ₁₁ N ₃ ·H ₂ O	[RuCl(C ₁₀ H ₁₄)(C ₂₇ H ₂₅ N ₃)] ⁺ ·PF ₆ ⁻
Formula weight	263.29	807.20
Temperature (K)	296	296
Wavelength (Å)	0.71073 Mo K α	0.71073 Mo K α
Crystal system	Triclinic	Triclinic
Space group	P-1 (No. 2)	P-1 (No. 2)
Unit cell parameters		
<i>a</i> , <i>b</i> , <i>c</i> (Å)	7.5935(5), 7.6012(5), 25.1873(17)	9.6358(4), 9.8169(4), 20.2513(8)
α , β , γ (°)	88.643(5), 88.691(5), 63.247(5)	75.804(3), 81.358(3), 83.621(3)
Volume (Å ³)	1297.70(16)	1830.54(13)
<i>Z</i>	4	2
<i>D</i> _{calc} (g/cm ³)	1.348	1.464
μ (mm ⁻¹)	0.087	0.606
Absorption correction	Integration	Integration
<i>T</i> _{min} , <i>T</i> _{max}	0.9788, 0.9952	0.8041, 0.9611
<i>F</i> ₀₀₀	552	824
Crystal size (mm ³)	0.54 × 0.48 × 0.15	0.45 × 0.22 × 0.07
Diffractometer/measurement method	STOE IPDS II/ ω scan	STOE IPDS II/ ω scan
Index ranges	-9 ≤ <i>h</i> ≤ 9, -9 ≤ <i>k</i> ≤ 9, -32 ≤ <i>l</i> ≤ 32	-12 ≤ <i>h</i> ≤ 12, -12 ≤ <i>k</i> ≤ 12, -26 ≤ <i>l</i> ≤ 26
θ range for data collection (°)	1.618 ≤ θ ≤ 27.166	2.092 ≤ θ ≤ 27.566
Reflections collected	17073	26026
Independent/observed reflections	5731/2785	8420/5195
<i>R</i> _{int}	0.086	0.1022
Refinement method	Full-matrix least-squares on <i>F</i> ²	Full-matrix least-squares on <i>F</i> ²
Data/restraints/parameters	5731/8/380	8420/52/481
Goodness-of-fit on <i>F</i> ²	1.063	1.017
Final <i>R</i> indices [<i>I</i> > 2σ(<i>I</i>)]	<i>R</i> ₁ = 0.1291, <i>wR</i> ₂ = 0.2797	<i>R</i> ₁ = 0.0822, <i>wR</i> ₂ = 0.2173
<i>R</i> indices (all data)	<i>R</i> ₁ = 0.1775, <i>wR</i> ₂ = 0.3063	<i>R</i> ₁ = 0.1236, <i>wR</i> ₂ = 0.2438
Δρ _{max} , Δρ _{min} (e/Å ³)	1.195, -0.295	1.680, -0.801

**Scheme 1.** Synthesis of compounds and numbering scheme for the NMR.

fragment of **L1** ($-H_3$ and $-H_6$) appeared as doublets at 7.63 and 7.77 ppm, respectively. The protons belonging quinoline moiety of **L1** appeared as doublet of doublet of doublets at 7.67 ppm for $-H_{13}$ and at 7.86 ppm for $-H_{14}$, as doublet of doublets at 8.06 ppm for $-H_{10}$ and at 8.17 ppm for $-H_9$; as doublet at 8.49 ppm for $-H_{12}$ and

at 8.54 ppm for $-H_{15}$. $-NH$ proton of **L1** was observed at 13.22 ppm as a broad singlet. The main difference in ¹H NMR spectra of **L2-5** from **L1** are loss of peak for $-NH$ proton and occurrence of new peaks belonging benzylic protons. $-H_a$ protons were monitored as singlet at 6.41 ppm for **L2**, at 6.49 ppm for **L3**, at 6.40 ppm for **L4**

and as multiplet between 6.28 and 6.42 ppm for **L5**. Other aromatic protons belonging benzylic group appeared around 6.28–8.88 ppm in **L2-5**.

The main difference in ^1H NMR spectra of **C1** compared to **L1** is the formation of new peaks belonging *p*-cymene groups. The protons belonging to *p*-cymene groups of **C1** appeared as doublet of doublets at 0.72 ppm for $-H_o$, as multiplet between 2.18 and 2.22 ppm for $-H_n$, as singlet at 2.29 ppm for $-H_k$, as doublet at 6.12 ppm for $-H_l$, as doublet at 6.26 ppm for $-H'$ and as doublet of doublets at 6.33 ppm for $-H_m$. Unusual peaks of $-H_{o,l,m}$ may be related with the symmetry of complexes. This phenomenon was supported by the ^{13}C NMR spectra of **C1**. There are six-singlet belonging to $-C_{o,l,m}$ in ^{13}C NMR spectra of **C1**. After the complexation, the protons belonging to quinoline and benzimidazol fragments of **L1** were generally shifted downfield. Surprisingly, there is no observed N–H proton in ^1H NMR spectra of **C1**. On the other hand, the measurement of ionic conductivity of **C1** shows that this compound has ionic nature. Due to the excess of the aromatic protons, the ^1H NMR spectra of **C2-5** were quite complicated. However, similar trends appeared in ^1H and ^{13}C NMR spectra of **C2-5**. The detailed assignment is given in the experimental section for all compounds.

In the FT-IR spectra of **L1**, N–H and $-\text{C}=\text{N}-$ stretching vibrations were observed at 3482 and 1619 cm^{-1} , respectively. The basic difference of **L2-5** from **L1** is loss of N–H stretch band and occurrence of aliphatic C–H stretching peaks belonging to benzylic group between 2973 and 2883 cm^{-1} . $-\text{C}=\text{N}-$ stretching vibrations of **L2-5** were observed at 1613, 1614, 1615, and 1612 cm^{-1} , respectively. After complexation, new vibrations belonging to cymene group were observed and $-\text{C}=\text{N}-$ stretching vibrations slightly shifted (1620 cm^{-1} for **C1**, 1616 cm^{-1} for **C2**, 1619 cm^{-1} for **C3**, 1641 cm^{-1} for **C4**, 1616 cm^{-1} for **C5**). Additionally, there is a broad band in the region between 3300 and 3100 cm^{-1} belonging to hydrated molecules on the FT-IR spectra of **C1-5**. Synthesized complexes have partially hygroscopic nature in solid-state.

In UV-VIS spectra of the ligands (**L1-5**), the peaks belonging to $\pi \rightarrow \pi^*$ and $n \rightarrow \pi^*$ transitions were appeared around 204–349 nm. A new charge transfer band occurred around 372–383 nm after complexation.

3.2. Description of the crystal structures

The solid-state structures of **L1** and **C3** have been clearly confirmed by single crystal X-ray analysis, even if their geometric parameters were not very accurate due to the high R -values. The perspective ORTEP-3 [44] views of **L1** and **C3** with the atomic numbering scheme are shown in Figs. 1(a) and 2(a), respectively, while selected bond lengths and angles are given in Table 2. Both compounds crystallize in the triclinic space group $P\bar{1}$ and there are two molecules in the asymmetric unit of **L1**, labeled as A and B. For the sake of clarity, only one (molecule A) of the two molecules is shown in Fig. 1(a). In the following discussion, parameters for molecule B are given in square brackets.

The molecule of **L1** consists of a benzimidazole ring with a quinoline ring in the 2-position of the benzimidazole and a water solvent molecule. The benzimidazole and quinoline rings of the molecule almost share a common plane with a dihedral angle of 3.4(2) $^\circ$ [3.7(3) $^\circ$]. In the benzimidazole ring, the N=C imine bond length of 1.288(8) \AA [1.265(8) \AA] is shorter than the amine N–C bond length of 1.349(8) \AA [1.393(7) \AA], as expected. The bond lengths and angles of **L1** exhibit no unusual features.

The cationic complex of **C3** is composed of a **L3** ligand with an Ru(II) metal center, one *p*-cymene ligand and one Cl ligand. The charge is neutralized by a hexafluorophosphate anion. The complex has the familiar half-sandwich “three-legged piano-stool”

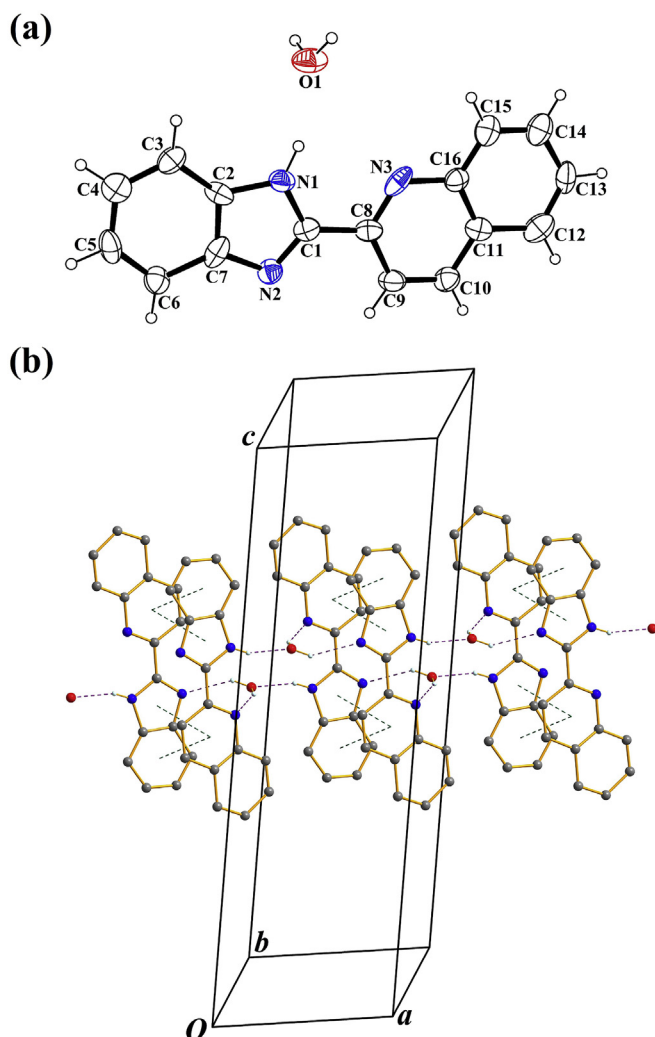


Fig. 1. (a) A view of **L1** showing the atom-numbering scheme. Displacement ellipsoids are drawn at the 30% probability level and H atoms are shown as small spheres of arbitrary radii. (b) Part of the crystal structure of **L1**, showing a molecular chain along [100]. For the sake of clarity, H atoms not involved in H-bonds have been omitted.

geometry with the η^6 π -bound arene ring forming the seat, and the two nitrogen atoms of the benzimidazole and quinoline rings of the **L3** and one terminal chloride ligand as the legs of the piano-stool.

The Ru(II) ion shows a pseudo-octahedral coordination geometry with the *p*-cymene formally occupying three facial coordination sites. However, the coordination geometry around the ruthenium can be regarded as a tetrahedron with considerable trigonal distortion, taking into account the center of the η^6 -*p*-cymene aromatic ring as the fourth ligand position. If X is defined as the centroid of the aromatic ring, the Ru–X distance is found to be 1.7021(5) \AA , and the Cl1–Ru1–X, N2–Ru1–X and N3–Ru1–X angles are 129.78(7), 128.69(16) and 133.52(13) $^\circ$, respectively. The Cl1–Ru1–N2, Cl1–Ru1–N3 and N2–Ru1–N3 angles [mean 81.91 $^\circ$] are smaller than the ideal tetrahedral angle (109.47 $^\circ$), which is counterbalanced by the extending of the X–Ru–L (L is Cl1, N2 or N3) angles [mean 130.66 $^\circ$]. Similar to related Ru(II)-arene complexes [22–30], there are substantial differences in the C–C [1.368(11)–1.483(17) \AA] and Ru–C [2.164(8)–2.233(9) \AA] distances for the arene ring. In the complex, the arene ring is planar with an r.m.s deviation from the plane of 0.0183 \AA . The two N-donor atoms of the bidentate ligand form a five-membered metallocycle

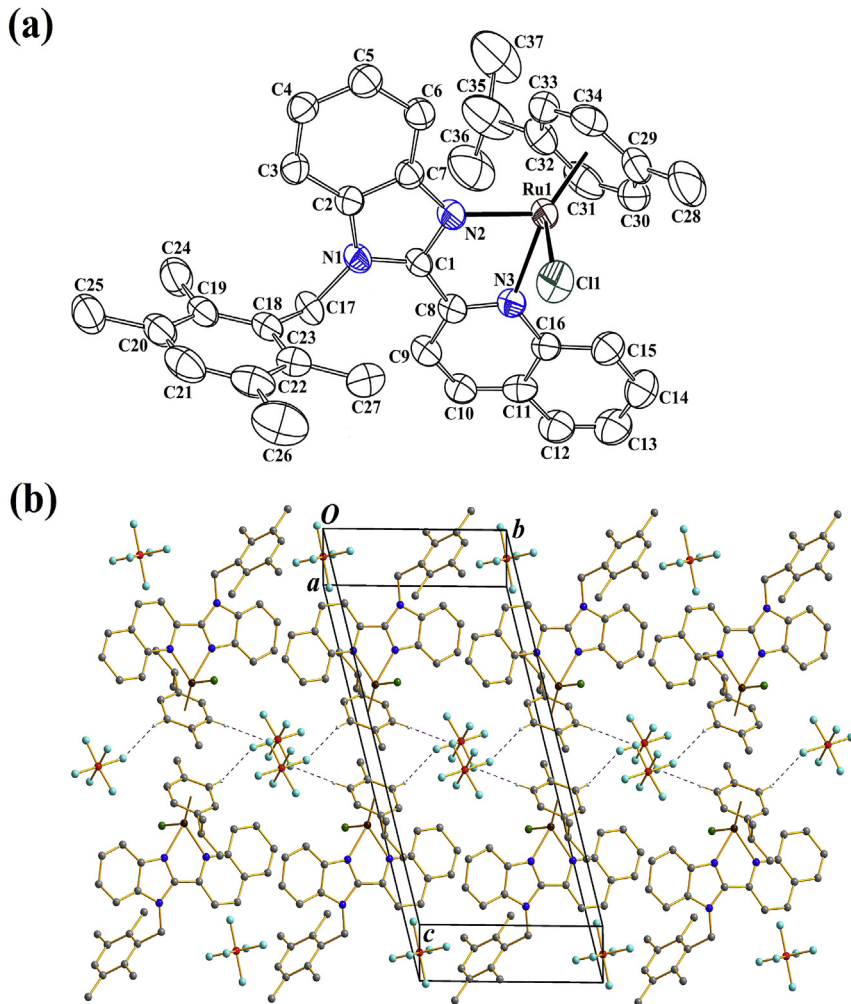


Fig. 2. (a) A view of **C3** showing the atom-numbering scheme. Displacement ellipsoids are drawn at the 30% probability level. The hexafluorophosphate anions and hydrogen atoms have been omitted for the sake of clarity. (b) Part of the crystal structure of **C3**, showing a molecular chain along [010]. For the sake of clarity, H atoms not involved in H-bonds have been omitted.

(containing atoms Ru1/N2/C1/C8/N3) with an r.m.s deviation from the plane being 0.0569 Å. The bond distances of Ru—Cl1, Ru1—N2 and Ru1—N3 are 2.380(2), 2.057(5) and 2.171(5) Å, respectively.

In the literature, many Ru(II)-arene complexes with the same coordination environment have been reported [16,47–54]. It is observed in these examples that the Ru—X, Ru—C, Ru—Cl and Ru—N bond lengths change from 1.674 to 1.704 Å, from 2.141 to 2.273 Å, from 2.385 to 2.432 Å and from 2.077 to 2.130 Å, respectively. As a result, the coordination bond distances are comparable with the literature values.

Partial packing diagrams of the compounds are shown in Figs. 1(b) and 2(b), while the geometric parameters belonging to the H-bonding interactions are given in Table 3. In the molecular structures of both compounds, no intramolecular interactions are observed. There are no intermolecular interactions between molecule A and molecule B in the crystal structure of **L1**, and both molecules have exactly the same pattern of H-bonding. In this pattern, the benzimidazole-quinoline molecule is connected to the water molecule by N—H···Cl interaction, while the water molecule acts as a hydrogen-bond donor to N2 and N3 atoms of the inversion-related molecules. There are also $\pi\cdots\pi$ stacking interactions between the benzimidazole and quinolone rings of these inversion-related molecules, centroid-centroid separations being

$Cg1\cdots Cg3 = 3.816(4)$ Å [3.814(4) Å], $Cg1\cdots Cg4 = 3.777(4)$ Å [3.731(5) Å], $Cg2\cdots Cg3 = 3.804(4)$ Å [3.844(5) Å] and $Cg2\cdots Cg4 = 3.901(4)$ Å [3.794(5) Å] ($Cg1 = N1/N2/C1/C2/C7$, $Cg2 = C2—C7$, $Cg3 = N3/C8—C11/C16$ and $Cg4 = C11—C16$). Together, these interactions form a molecular chain running parallel to [100] direction for molecule A, and a molecular chain running parallel to [010] direction for molecule B. In the crystal structure of **C3**, the molecules are linked to each other by means of two C—H···F interactions, generating a molecular chain along the *b* axis.

3.3. Catalytic studies

Synthesized Ru(II) complexes (**C1–5**) were tested as catalysts in selective oxidation of benzyl alcohol to benzaldehyde. Preliminary catalytic reactions were performed with **C1**. First, the ratios of substrat/catalyst/oxidant (*S/C/O*) as 1/0.01/0.5 were chosen. Then, different solvents were tested to determine the optimum reaction conditions (Fig. 3). Maximum activity was observed in acetonitrile as solvent. No oxidation reaction occurred in the absence of catalyst with H_5IO_6 as oxidant. The catalytic reaction becomes notably slower at room temperature (after 1 h–8%). According to preliminary results, **C1–5** (0.01 mmol), periodic acid (0.5 mmol) and benzyl alcohol (1 mmol) were refluxed at 82 °C in CH_3CN (5 mL)

Table 2
Selected geometric parameters for **L1** and **C3**.

Parameter	L1		C3
	Molecule A	Molecule B	
Bond lengths (Å)			
Ru1–Cl1	—	—	2.380(2)
Ru1–N2	—	—	2.057(5)
Ru1–N3	—	—	2.171(5)
Ru1–C29	—	—	2.231(8)
Ru1–C30	—	—	2.221(8)
Ru1–C31	—	—	2.164(8)
Ru1–C32	—	—	2.233(9)
Ru1–C33	—	—	2.180(8)
Ru1–C34	—	—	2.176(7)
N1–C1	1.349(8)	1.393(7)	1.368(8)
N1–C2	1.427(9)	1.408(9)	1.409(7)
N1–C17	—	—	1.468(8)
N2–C1	1.288(8)	1.265(8)	1.322(8)
N2–C7	1.368(7)	1.367(8)	1.378(8)
N3–C8	1.320(9)	1.275(8)	1.315(8)
N3–C16	1.425(9)	1.454(9)	1.381(8)
C1–C8	1.467(9)	1.520(9)	1.456(8)
C17–C18	—	—	1.523(8)
Bond angles (°)			
Cl1–Ru1–N2	—	—	85.47(16)
Cl1–Ru1–N3	—	—	85.26(15)
Cl1–Ru1–C29	—	—	90.1(3)
Cl1–Ru1–C30	—	—	110.3(4)
Cl1–Ru1–C31	—	—	147.8(4)
Cl1–Ru1–C32	—	—	166.0(2)
Cl1–Ru1–C33	—	—	130.0(2)
Cl1–Ru1–C34	—	—	99.6(2)
N2–Ru1–N3	—	—	75.0(2)
N2–Ru1–C29	—	—	146.5(4)
N2–Ru1–C30	—	—	164.2(4)
N2–Ru1–C31	—	—	125.4(4)
N2–Ru1–C32	—	—	96.3(3)
N2–Ru1–C33	—	—	91.8(3)
N2–Ru1–C34	—	—	112.0(3)
N3–Ru1–C29	—	—	137.7(3)
N3–Ru1–C30	—	—	107.0(3)
N3–Ru1–C31	—	—	93.9(3)
N3–Ru1–C32	—	—	108.6(3)
N3–Ru1–C33	—	—	141.9(3)
N3–Ru1–C34	—	—	171.6(3)
N1–C1–N2	113.1(6)	117.4(6)	112.0(5)
C1–N1–C2	107.2(5)	104.9(5)	105.5(5)
C1–N2–C7	104.9(6)	101.2(5)	107.5(5)
C1–N1–C17	—	—	128.7(5)
C2–N1–C17	—	—	124.8(5)
C8–N3–C16	118.1(6)	122.1(5)	119.0(5)
N1–C1–C8	121.8(6)	116.8(5)	131.2(5)
N2–C1–C8	125.0(6)	125.8(5)	116.9(5)
N1–C17–C18	—	—	113.9(5)
N3–C8–C1	115.8(6)	117.5(5)	113.0(5)
N1–C2–C7	101.7(6)	100.7(6)	106.8(5)
N2–C7–C2	112.8(7)	115.3(6)	108.2(5)

(Fig. 4). Under these conditions, we show that benzaldehyde occurs as a single product.

In conclusion, the results show that **C2** is a more active catalyst than the others. After 1 h, **C1** has lower catalytic activity than **C2–5**. These results have shown that the efficiency of the catalyst seems to depend not only on the quinolinyl-benzimidazole fragment of the ligands but also on the benzyl fragment of the ligands. Interestingly, catalytic activity decreases when methyl or chlorine groups are introduced to the benzyl fragment. These results show that easily synthesized these complexes are moderately active catalysts in the oxidation of benzyl alcohol to benzaldehyde in the presence of periodic acid. A plausible mechanism may be proposed for this reaction (Fig. 5). Some studies suggest that an initial carbonyl-bound Ru(IV) species is generated upon reaction with

Table 3
Hydrogen bonding geometry for **L1** and **C3**.

D–H···A	D–H (Å)	H···A (Å)	D···A (Å)	D–H···A (°)
L1				
N1B–H1B···O1B	0.86(1)	1.93(2)	2.760(7)	163(6)
O1B–H1B1···N2B ^a	0.82(1)	2.00(3)	2.793(7)	162(8)
N1A–H1A···O1A	0.86(1)	1.96(2)	2.780(7)	160(6)
O1A–H2A1···N3A ^b	0.82(1)	2.31(3)	3.069(8)	153(6)
O1A–H1A1···N2A ^c	0.82(1)	2.12(5)	2.828(7)	145(8)
O1B–H2B1···N3B ^d	0.82(1)	2.35(4)	3.056(7)	145(6)
C3				
C34–H34···F8 ^e	0.93	2.49	3.409(14)	169
C30–H30···F6 ^f	0.93	2.45	3.045(12)	122

Symmetry codes.

- ^a $x, y+1, z$.
- ^b $-x+2, -y+2, -z+1$.
- ^c $x+1, y, z$.
- ^d $-x+2, -y+1, -z$.
- ^e $-x+1, -y+1, -z+1$.
- ^f $-x+1, -y, -z+1$.

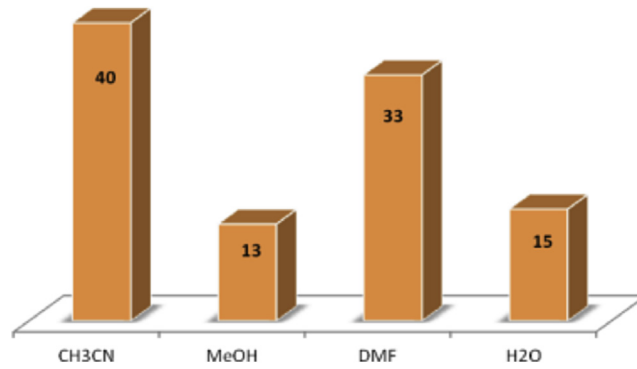


Fig. 3. The oxidation of benzyl alcohol to benzaldehyde using different solvents in the presence of **C1** as catalyst and H₅IO₆ as oxidant at 82 °C in CH₃CN (the ratio of S/C/H₅IO₆ is 1/0.01/0.5).

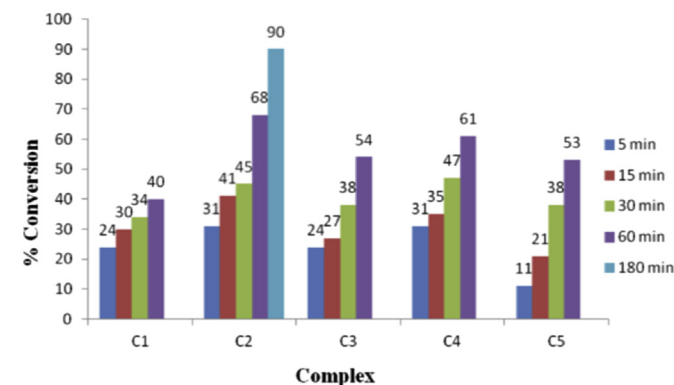


Fig. 4. The oxidation of benzyl alcohol to benzaldehyde using **C1–5** at 82 °C in acetonitrile (the ratio of S/C/H₅IO₆ is 1/0.01/0.5).

periodic acid and concomitant loss of water molecules. The loaded catalysts then regenerate and initiate a second catalytic cycle [40,55].

4. Conclusion

In this work, five bidentate quinolinyl-benzimidazole ligands (**L1–5**) and their heteroleptic Ru(II) complexes (**C1–5**) were synthesized and characterized with IR, UV–vis and NMR techniques.

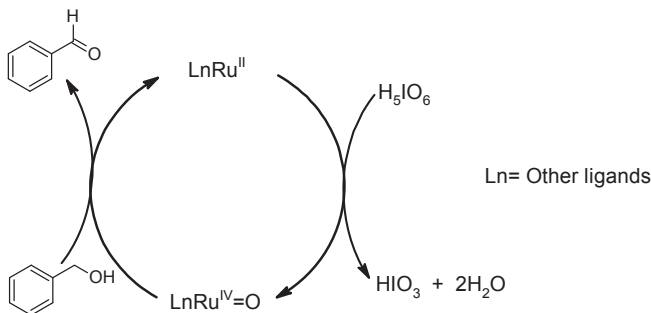


Fig. 5. Proposed mechanism for oxidation of benzyl alcohol to benzaldehyde-catalyzed ruthenium complexes in the presence of H_5IO_6 .

Single-crystal X-ray diffraction studies show that solid state structures of **L1** and **C3** completely agree with proposed structures. In **C3**, there is a distorted octahedral environment around the central metal ions. Ruthenium atom is coordinated by bidentate **L3**, η^6 π -bound *p*-cymene ring and one terminal chloride ligand. Cationic complex ions are neutralized with PF_6^- anion. Synthesized complexes were tested as catalysts in the oxidation of benzyl alcohol to benzaldehyde in the presence of H_5IO_6 . Results show that all complexes are moderately active in this reaction. **C2–5** complexes including benzyl-framework are more efficient than **C1**. The order of catalytic efficiency is **C2>C4>C3>C5>C1**. The higher catalytic efficiency of **C2** compared to the others may be related with steric parameters. Additionally, benzylic protons may play an important role in the catalytic cycle.

Acknowledgements

We acknowledge Çanakkale Onsekiz Mart University Scientific Research Projects Commission (Project No: FBA-2014-179) for support and the Faculty of Arts and Sciences, Ondokuz Mayıs University, Turkey, for the use of the STOE IPDS II diffractometer (purchased under grant No. F-279 of the University Research Fund).

Appendix A. Supplementary data

CCDC 1036751 and 1036752 contain the supplementary crystallographic data for the compounds reported in this article. These data can be obtained free of charge via <http://www.ccdc.cam.ac.uk/conts/retrieving.html>, or from the Cambridge Crystallographic Data Centre, 12 Union Road, Cambridge CB2 1EZ, UK; fax: (+44) 1223-336-033; or e-mail: deposit@ccdc.cam.ac.uk. Supplementary data related to this article can be found at <http://dx.doi.org/10.1016/j.molstruc.2016.06.017>.

References

- [1] H. Kucukbay, B. Cetinkaya, S. Guesmi, P.H. Dixneuf, New (carbene)ruthenium-arene complexes: preparation and uses in catalytic synthesis of furans, *Organometallics* 15 (1996) 2434–2439.
- [2] S. Dayan, N.O. Kalaycioglu, J.C. Daran, A. Labande, R. Poli, Synthesis and characterization of half-sandwich ruthenium complexes containing aromatic sulfonamides bearing pyridinyl rings: catalysts for transfer hydrogenation of acetophenone derivatives, *Eur. J. Inorg. Chem.*, DOI 10.1002/ejic.201300266(2013) 3224–3232.
- [3] S. Koya, Y. Nishioka, H. Mizoguchi, T. Uchida, T. Katsuki, Asymmetric epoxidation of conjugated olefins with dioxygen, *Angew. Chemie-International Ed.* 51 (2012) 8243–8246.
- [4] J.J. Concepcion, M.K. Tsai, J.T. Muckerman, T.J. Meyer, Mechanism of water oxidation by single-site ruthenium complex catalysts, *J. Am. Chem. Soc.* 132 (2010) 1545–1557.
- [5] Q.F. Wang, W.M. Du, T.T. Liu, H.N. Chai, Z.K. Yu, Ruthenium(II)-NNN complex catalyzed Oppenauer-type oxidation of secondary alcohols, *Tetrahedron Lett.* 55 (2014) 1585–1588.
- [6] J.G. Malecki, A. Maron, S. Krompiec, M. Filapek, M. Penkala, B. Marcel, Synthesis, characterizations and catalytic applications of hydridecarbonyl ruthenium(II) complexes with imidazole carboxylic acid derivative ligands, *Polyhedron* 49 (2013) 190–199.
- [7] X. Ma, X. Li, Y.E. Cha, L.P. Jin, Highly thermostable one-dimensional lanthanide(III) coordination polymers constructed from benzimidazole-5,6-dicarboxylic acid and 1,10-Phenanthroline: synthesis, structure, and tunable white-light emission, *Cryst. Growth Des.* 12 (2012) 5227–5232.
- [8] S. Samai, K. Biradha, Chemical and mechano responsive metal-organic gels of bis(benzimidazole)-based ligands with Cd(II) and Cu(II) halide salts: self sustainability and gas and dye sorptions, *Chem. Mater.* 24 (2012) 1165–1173.
- [9] V.C.O. Njar, A.M.H. Brodie, Discovery and development of galerone (TOK-001 or VN124-1) for the treatment of all stages of prostate cancer, *J. Med. Chem.* 58 (2015) 2077–2087.
- [10] Y. Bansal, O. Silakari, The therapeutic journey of benzimidazoles: a review, *Bioorgan. Med. Chem.* 20 (2012) 6208–6236.
- [11] Y.L. Yao, Y.X. Che, J.M. Zheng, The coordination chemistry of benzimidazole-5,6-dicarboxylic acid with Mn(II), Ni(II), and Ln(III) complexes ($\text{Ln} = \text{Tb}, \text{Ho}, \text{Er}, \text{Lu}$), *Cryst. Growth Des.* 8 (2008) 2299–2306.
- [12] C.H. Chen, W.S. Huang, M.Y. Lai, W.C. Tsao, J.T. Lin, Y.H. Wu, T.H. Ke, L.Y. Chen, C.C. Wu, Versatile benzimidazole/amine-based ambipolar compounds for electroluminescent applications: single-layer, blue, fluorescent OLEDs, hosts for single-layer, phosphorescent OLEDs, *Adv. Funct. Mater.* 19 (2009) 2661–2670.
- [13] G.G. Mohamed, Z.H. Abd El-Wahab, Salicylidene-2-aminobenzimidazole Schiff base complexes of Fe(III), Co(II), Ni(II), Cu(II), Zn(II) and Cd(II), *J. Therm. Anal. Calorim.* 73 (2003) 347–359.
- [14] M.R. Maurya, A. Kumar, M. Ebel, D. Rehder, Synthesis, characterization, reactivity, and catalytic potential of model vanadium(IV, V) complexes with benzimidazole-derived ONN donor ligands, *Inorg. Chem.* 45 (2006) 5924–5937.
- [15] M.R. Maurya, M. Bisht, A. Kumar, M.L. Kuznetsov, F. Avecilla, J.C. Pessoa, Synthesis, characterization, reactivity and catalytic activity of oxidovanadium(IV), oxidovanadium(V) and dioxidovanadium(V) complexes of benzimidazole modified ligands, *Dalton T* 40 (2011) 6968–6983.
- [16] O. Dayan, S. Demirmen, N. Ozdemir, Heteroleptic ruthenium(II) complexes of 2-(2-pyridyl)benzimidazoles: a study of catalytic efficiency towards transfer hydrogenation of acetophenone, *Polyhedron* 85 (2015) 926–932.
- [17] O. Dayan, N. Ozdemir, Z. Serbetci, M. Dincer, B. Cetinkaya, O. Buyukgunor, Synthesis and catalytic activity of ruthenium(II) complexes containing pyridine-based tridentate triamines ('NNN') and pyridine carboxylate ligands (NO), *Inorg. Chim. Acta* 392 (2012) 246–253.
- [18] O. Dayan, S. Dayan, I. Kani, B. Cetinkaya, Ruthenium(II) complexes bearing pyridine-based tridentate and bidentate ligands: catalytic activity for transfer hydrogenation of aryl ketones, *Appl. Organomet. Chem.* 26 (2012) 663–670.
- [19] N.M. Shavaleev, S.V. Eliseeva, R. Scopelliti, J.C.G. Bunzli, Designing simple tridentate ligands for highly luminescent europium complexes, *Chem-Eur J.* 15 (2009) 10790–10802.
- [20] Q.Y. Yu, B.X. Lei, J.M. Liu, Y. Shen, L.M. Xiao, R.L. Qiu, D.B. Kuang, C.Y. Su, Ruthenium dyes with heteroleptic tridentate 2,6-bis(benzimidazol-2-yl)-pyridine for dye-sensitized solar cells: enhancement in performance through structural modifications, *Inorg. Chim. Acta* 392 (2012) 388–395.
- [21] A.K. Vannucci, J.F. Hull, Z. Chen, R.A. Binstead, J.J. Concepcion, T.J. Meyer, Water oxidation intermediates applied to catalysis: benzyl alcohol oxidation, *J. Am. Chem. Soc.* 134 (2012) 3972–3975.
- [22] J. Diez, J. Gimeno, A. Lledos, F.J. Suarez, C. Vicent, Imidazole based ruthenium(IV) complexes as highly efficient bifunctional catalysts for the redox isomerization of allylic alcohols in aqueous medium: water as cooperating ligand, *Acs Catal.* 2 (2012) 2087–2099.
- [23] W.J. Ye, M. Zhao, W.M. Du, Q.B. Jiang, K.K. Wu, P. Wu, Z.K. Yu, Highly active ruthenium(II) complex catalysts bearing an unsymmetrical NNN ligand in the (asymmetric) transfer hydrogenation of ketones, *Chem-Eur J.* 17 (2011) 4737–4741.
- [24] J. Zhou, Z.G. Lu, G.G. Shan, S.H. Wang, Y. Liao, Gadolinium complex and phosphorescent probe-modified NaDyF4 nanorods for T-1 and T-2-weighted MRI/CT/phosphorescence multimodality imaging, *Biomaterials* 35 (2014) 368–377.
- [25] W.J. Zhang, W. Huang, T.L. Liang, W.H. Sun, Half-Titanocene chlorides 2-(benzimidazol-2-yl)quinolin-8-olates: synthesis, characterization and ethylene (co-)polymerization behavior, *Chin. J. Polym. Sci.* 31 (2013) 601–609.
- [26] S. Li, B. Zhang, F.E. Kuhn, Benzimidazolic complexes of methyltrioxorhenium(VII): synthesis and application in catalytic olefin epoxidation, *J. Organomet. Chem.* 730 (2013) 132–136.
- [27] J.J. Xia, Z.H. Zhou, W. Li, H.Q. Zhang, C. Redshaw, W.H. Sun, Synthesis, structure and fluorescent properties of 2-(1H-benzimidazol-2-yl)quinolin-8-ol ligands and their zinc complexes, *Inorg. Chim. Acta* 394 (2013) 569–575.
- [28] F. He, X. Hao, X.P. Cao, C. Redshaw, W.H. Sun, Nickel halide complexes bearing 2-benzimidazolyl-N-arylquinoline-8-carboxamide derived ligands: synthesis, characterization and catalytic behavior towards ethylene oligomerization and the vinyl polymerization of norbornene, *J. Organomet. Chem.* 712 (2012) 46–51.
- [29] J.H. Min, Q.S. Zhang, W. Sun, Y.X. Cheng, L.X. Wang, Neutral copper(I) phosphorescent complexes from their ionic counterparts with 2-(2'-quinolyl)

- benzimidazole and phosphine mixed ligands, *Dalton T* 40 (2011) 686–693.
- [30] S.J. Li, Y. Li, Synthesis and properties of a novel ruthenium complex containing a 2-(benzimidazol-2-yl)-8-octyloxyquinoline tridentate ligand, *Inorg. Chem. Commun.* 14 (2011) 683–685.
- [31] L. He, J. Qiao, L. Duan, G.F. Dong, D.Q. Zhang, L.D. Wang, Y. Qiu, Toward highly efficient solid-state white light-emitting electrochemical cells: blue-green to red emitting cationic iridium complexes with imidazole-type ancillary ligands, *Adv. Funct. Mater.* 19 (2009) 2950–2960.
- [32] A.J. Hallett, B.D. Ward, B.M. Kariuki, S.J.A. Pope, Neutral and cationic cyclo-metallated Ir(III) complexes of anthra[1,2-d]-imidazole-6,11-dione-derived ligands: syntheses, structures and spectroscopic characterisation, *J. Organomet. Chem.* 695 (2010) 2401–2409.
- [33] Z.C. Zhu, M. Kojima, K. Nakajima, Reversible ring opening and closure reactions of the triazine ligands derived from 1-phenylazo-2-naphthylamine and pyridine-2-aldehyde or quinoline-2-aldehyde structure and reactivity of the palladium(II) complexes, *Inorg. Chim. Acta* 358 (2005) 476–488.
- [34] M.L. Guo, H.Z. Li, Selective oxidation of benzyl alcohol to benzaldehyde with hydrogen peroxide over tetra-alkylpyridinium octamolybdate catalysts, *Green Chem.* 9 (2007) 421–423.
- [35] S. Dayan, A. Cetin, N.B. Arslan, N.K. Ozpozan, N. Ozdemir, O. Dayan, Palladium(II) complexes bearing bidentate pyridyl-sulfonamide ligands: synthesis and catalytic applications, *Polyhedron* 85 (2015) 748–753.
- [36] G. Wu, Y. Gao, F.W. Ma, B.H. Zheng, L.G. Liu, H.Y. Sun, W. Wu, Catalytic oxidation of benzyl alcohol over manganese oxide supported on MCM-41 zeolite, *Chem. Eng. J.* 271 (2015) 14–22.
- [37] A. Kumar, B. Sreedhar, K.V.R. Chary, Highly dispersed gold nanoparticles supported on SBA-15 for vapor phase aerobic oxidation of benzyl alcohol, *J. Nanosci. Nanotechno* 15 (2015) 1714–1724.
- [38] L.F. Nascimento, E.Y. Matsubara, P.M. Donate, J.M. Rosolen, Catalytic behavior of ruthenium anchored on micronanostructured composite in selective benzyl alcohol oxidation, *React. Kinet. Mech. Cat.* 110 (2013) 471–483.
- [39] S. Dayan, N.O. Kalaycioglu, Synthesis, characterization and catalytic properties of novel palladium(II) complexes containing aromatic sulfonamides: effective catalysts for the oxidation of benzyl alcohol, *Appl. Organomet. Chem.* 27 (2013) 52–58.
- [40] Z.M. Hu, L. Ma, J.H. Xie, H.X. Du, W.W.Y. Lam, T.C. Lau, Ruthenium-catalyzed oxidation of alcohols by bromate in water, *New J. Chem.* 37 (2013) 1707–1710.
- [41] M. Murali, R. Mayilmurugan, M. Palaniandavar, Synthesis, structure and spectral, and electrochemical properties of new mononuclear ruthenium(III) complexes of tris[(benzimidazol-2-yl)methyl]amine: role of steric hindrance in tuning the catalytic oxidation activity, *Eur. J. Inorg. Chem.*, DOI 10.1002/ejic.200900119 (2009) 3238–3249.
- [42] T.R. Chen, Synthesis, structure, and field-effect property of 2-(benzimidazol-2-yl)quinoline, *Mater. Lett.* 59 (2005) 1050–1052.
- [43] G.M. Sheldrick, A short history of SHELX, *Acta Crystallogr. A* 64 (2008) 112–122.
- [44] L.J. Farrugia, WinGX and ORTEP for windows: an update, *J. Appl. Crystallogr.* 45 (2012) 849–854.
- [45] Stoe, X.-A.R.E.A. Cie, Version 1.18 and X-RED32 Version 1.04, Stoe & Cie, Germany, Darmstadt, 2002.
- [46] A.L. Spek, Structure validation in chemical crystallography, *Acta Crystallogr. D* 65 (2009) 148–155.
- [47] D.L. Davies, J. Fawcett, S.A. Garratt, D.R. Russell, (Arene)ruthenium complexes with bis(oxazolines): synthesis and applications as asymmetric catalysts for Diels-Alder reactions, *Organometallics* 20 (2001) 3029–3034.
- [48] J.W. Faller, A. Lavoie, Highly enantioselective Diels-Alder catalysis with a chiral ruthenium bisoxazoline complex, *J. Organomet. Chem.* 630 (2001) 17–22.
- [49] R. Lalrempuia, M.R. Kollipara, Reactivity studies of eta(6)-arene ruthenium (II) dimers with polypyridyl ligands: isolation of mono, binuclear p-cymene ruthenium (II) complexes and bisterpyridine ruthenium (II) complexes, *Polyhedron* 22 (2003) 3155–3160.
- [50] W.B. Yao, K. Kavallieratos, S. de Gala, R.H. Crabtree, Dipyrimidylamine and tripyrimidylamine as chelating N-donor ligands, *Inorg. Chim. Acta* 311 (2000) 45–49.
- [51] J.X. Ong, C.W. Yap, W.H. Ang, Rational design of selective organoruthenium inhibitors of protein tyrosine phosphatase 1B, *Inorg. Chem.* 51 (2012) 12483–12492.
- [52] K.C. Cheung, W.L. Wong, M.H. So, Z.Y. Zhou, S.C. Yan, K.Y. Wong, A dinuclear ruthenium catalyst with a confined cavity: selectivity in the addition of aliphatic carboxylic acids to phenylacetylene, *Chem. Commun.* 49 (2013) 710–712.
- [53] C.A. Vock, C. Scolaro, A.D. Phillips, R. Scopelliti, G. Sava, P.J. Dyson, Synthesis, characterization, and in vitro evaluation of novel ruthenium(II) eta(6)-arene imidazole complexes, *J. Med. Chem.* 49 (2006) 5552–5561.
- [54] R.R. Dykeman, K.L. Luska, M.E. Thibault, M.D. Jones, M. Schlaf, M. Khanfar, N.J. Taylor, J.F. Britten, L. Harrington, Catalytic deoxygenation of terminal-diols under acidic aqueous conditions by the ruthenium complexes [(eta(6)-arene) Ru(X)(N boolean AND N)](OTf)(n), X = H₂O, H, eta(6)-arene = p-Me-Pr-i-C₆H₄, C₆Me₆, N boolean AND N = bipy, phen, 6,6'-diamino-bipy, 2,9-diamino-phen, n=1, 2) influence of the ortho-amine substituents on catalytic activity, *J. Mol. Catal. a-Chem* 277 (2007) 233–251.
- [55] S. Ganeshamoorthy, K. Shanmugasundaram, R. Karvembu, Mild oxidation of alcohols with periodic acid catalyzed by [Ru(acac)(2)(CH₃CN)(2)]PF₆ in water, *Catal. Commun.* 10 (2009) 1835–1838.